

# Pose Anything: A Graph-Based Approach for Category-Agnostic Pose Estimation

Or Hirschorn      Shai Avidan

Tel Aviv University

<https://orhir.github.io/pose-anything/>

## Abstract

Traditional 2D pose estimation models are limited by their category-specific design, making them suitable only for predefined object categories. This restriction becomes particularly challenging when dealing with novel objects due to the lack of relevant training data.

To address this limitation, category-agnostic pose estimation (CAPE) was introduced. CAPE aims to enable keypoint localization for arbitrary object categories using a single model, requiring minimal support images with annotated keypoints. This approach not only enables object pose generation based on arbitrary keypoint definitions but also significantly reduces the associated costs, paving the way for versatile and adaptable pose estimation applications.

We present a novel approach to CAPE that leverages the inherent geometrical relations between keypoints through a newly designed Graph Transformer Decoder. By capturing and incorporating this crucial structural information, our method enhances the accuracy of keypoint localization, marking a significant departure from conventional CAPE techniques that treat keypoints as isolated entities.

We validate our approach on the MP-100 benchmark, a comprehensive dataset comprising over 20,000 images spanning more than 100 categories. Our method outperforms the prior state-of-the-art by substantial margins, achieving remarkable improvements of 2.16% and 1.82% under 1-shot and 5-shot settings, respectively. Furthermore, our method’s end-to-end training demonstrates both scalability and efficiency compared to previous CAPE approaches.

## 1. Introduction

2D pose estimation, also known as keypoint localization, has recently gained significant prominence in computer vision research, finding diverse applications in both academic and industrial domains. This task involves predicting spe-

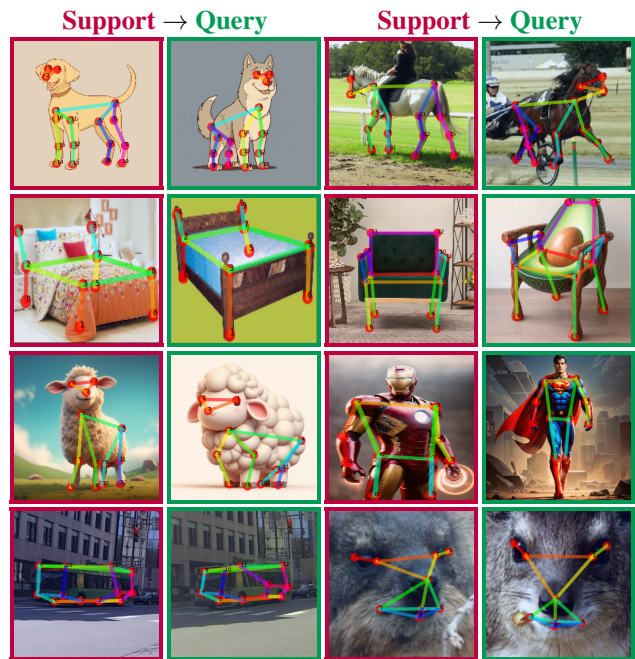


Figure 1. **Pose Anything.** Given a support image and skeleton from any category (purple) our model localizes the skeleton on a query image (green). Our graph-oriented category-agnostic pose estimation method integrates structural information to improve keypoint localization. Model was trained on one group of object classes and tested on different classes. Test set results are shown here.

cific semantic parts’ locations within an object depicted in an image. Notably, it plays a crucial role in areas such as human pose estimation for video understanding or virtual reality, animal pose estimation in zoology, and vehicle pose estimation for autonomous driving.

However, a fundamental limitation of conventional pose estimation models is their inherent category specificity. These models are typically designed to work exclusively within a predefined object category, restricting their use to

the domain they were trained on. Consequently, their adaptability to real-world situations involving novel objects is impeded due to the absence of relevant training data.

To address this challenge, category-agnostic pose estimation (CAPE) was proposed [42]. CAPE seeks to perform keypoint localization for arbitrary object categories, using a single model, by utilizing just one or a few support images with keypoint annotations, referred to as support keypoints. This approach enables the generation of an object’s pose based on arbitrary keypoint definitions. Significantly, it substantially reduces the extensive costs associated with data collection, model training, and parameter tuning for each novel class. This paves the way for more versatile and adaptable applications in the field of pose estimation. Figure 1 shows some results of our work.

Current CAPE methods match support keypoints with their corresponding counterparts in the query image. The matching is done in latent space to facilitate the localization of keypoints. One notable distinction from previous CAPE methods lies in their treatment of keypoints as individual, disconnected points. In contrast to these approaches, we recognize the significance of the underlying geometrical structure of objects. This structure serves as a robust prior that can significantly enhance the accuracy of keypoint localization. Building upon this realization, we introduce a novel Graph Transformer Decoder, purposefully designed to capture and incorporate this crucial structural information. By doing so, we aim to exploit the inherent relationships and dependencies between keypoints.

We evaluate our method on the category-agnostic pose estimation benchmark MP-100 [42]. This dataset contains over  $20k$  images from over 100 categories, including animals, vehicles, furniture, and clothes. It is composed of samples collected from existing category-specific pose estimation datasets. As some of the skeleton data was missing, we collected skeleton annotations from the original datasets and annotated several categories with missing skeleton definitions.

Our method outperforms the previous best approach CapeFormer [32] by large margins, with an improvement of 2.16% and 1.82% under 1-shot and 5-shot settings, respectively. Our method is trained end-to-end and demonstrates both scalability and efficiency compared with previous approaches.

To summarize, we propose three key contributions:

- We introduced a new method, leveraging the geometrical relations between keypoints using a novel Graph Transformer Decoder.
- We provide an updated version of the MP-100 dataset with skeleton annotations for all categories.
- State-of-the-art performance on the MP-100 benchmark.

## 2. Related Works

### 2.1. Detection Transformer

The DEtection TRansformer (DETR) [3] stands out for its simplicity and conceptually straightforward and universally applicable approach, requiring minimal domain-specific knowledge, and avoiding the need for customized label assignments or non-maximum suppression.

However, the original DETR design suffers from challenges such as slow convergence rates and reduced detection accuracy. In response, a multitude of subsequent studies, including [7, 11, 20, 24, 50, 53], have emerged, improving the DETR paradigm. These works have paved the way for the development of top-tier object detectors, leveraging innovations like the reintroduction of multi-scale features and local cross-attention computations [9, 39, 50].

A compelling connection emerges between detection problems, focused on bounding box estimation and localization, and pose estimation, which centers on keypoint localization. Recognizing this connection, we incorporate several advancements from the DETR model into the latest category-agnostic pose estimation method [32], thus improving its performance.

### 2.2. Category-Agnostic Pose Estimation

The primary goal of pose estimation is to accurately localize the semantic keypoints of objects or instances. Traditionally, pose estimation methods have predominantly been tailored to specific categories, such as humans [2, 8, 46], animals [48, 49], or vehicles [29, 34]. Existing research focused mainly on designing powerful convolutional neural networks [2, 8, 16] or transformer-based architectures [23, 43]. However, these methods are limited to object categories encountered during training.

A relatively unexplored facet is category-agnostic pose estimation, introduced by POMNet [42], where the emphasis shifts towards constructing a generic representation and similarity metrics. This approach predicts keypoints by comparing support keypoints with query images in the embedding space, addressing the challenge of object categories not seen during training.

POMNet [42] employs a transformer to encode query images and support keypoints, with a regression head predicting similarity directly from the concatenation of support keypoint and query image features. CapeFormer [33] extends the matching paradigm to a two-stage framework, rectifying unreliable matching outcomes to enhance prediction precision. We follow CapeFormer, enhancing their methodology with a more robust baseline. Moreover, we focus on the importance of geometrical structure, seamlessly integrating it into our architectural framework.

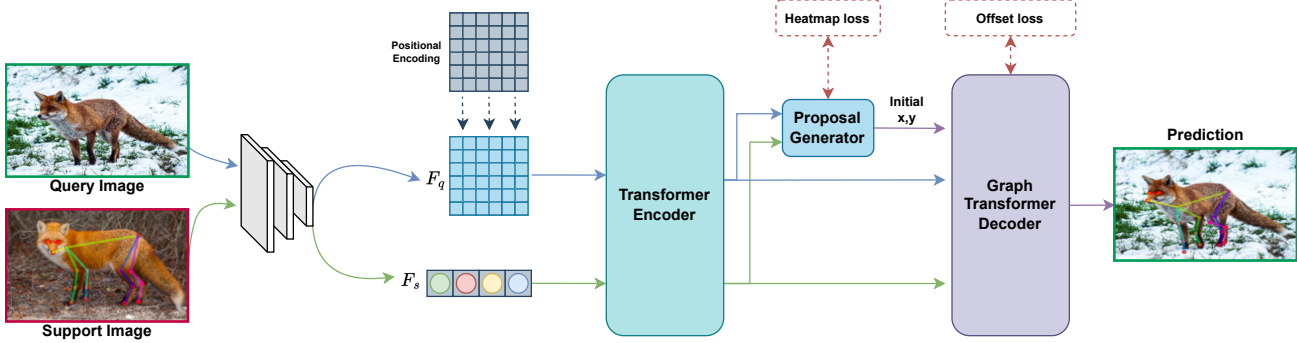


Figure 2. **Architecture Overview.** Our approach utilizes a pre-trained backbone to extract image features, followed by a transformer encoder that refines these features through self-attention. A similarity proposal generator is employed alongside a graph transformer decoder, enhancing keypoint localization accuracy with a focus on graph-oriented decoding.

### 2.3. Graph Neural Network

Originally designed for graph data like social networks [12], citation networks [30], and biochemical graphs [37], GCNs are gaining traction in computer vision tasks [15, 17, 38, 41]. They find a variety of applications such as scene graph generation, point cloud classification, and action recognition. Scene graph generation involves parsing images into graphs that represent objects and their relations, often combined with object detection [41, 45]. Point clouds, derived from LiDAR scans, are effectively classified and segmented using GCNs [17, 40]. Furthermore, GCNs have been employed for human activity recognition by processing naturally constructed graphs of human joints [5, 21, 44]. Recent work even suggests using GNNs as backbone feature extractors for visual tasks, representing images as graph structures [13].

In contrast to GCNs, which uniformly aggregate neighbor information based on the adjacency matrix, Graph Attention Networks (GAT)[36] introduce the concept of self-attention. GAT incorporates the graph structure into the attention mechanism through masked attention. Similarly, aGCN[45] relies on self-attention to determine the weights of neighboring joints, with differences arising from their choice of activation functions and transformation matrices. While GAT and aGCN advance the aggregation of neighbor joints, the challenge of limited receptive fields persists. Zhao *et al.* [51] addressed this limitation by introducing a learnable weighting matrix to the adjacency matrix, enabling the learning of semantic relationships between 2D joints. Similarly, Lin *et al.*[19] leveraged a standard transformer encoder by making adjustments to the dimension of encoder layers. However, these approaches, as previously mentioned, fail to fully exploit the inherent graph structure. In an attempt to address this challenge, Graformer [52] suggested a solution involving a combination of attention blocks followed by graph convolutions that employ learn-

able adjacency matrices. Nevertheless, their approach is primarily tailored for domain-specific applications, making it less suitable for our category-agnostic task.

Our category-agnostic method tackles this challenge by integrating both self-attention and a GCN network into the decoder’s architecture. Self-attention promotes learnable connections between keypoints, while the GCN, using the input from the skeleton graph, aids the model in sharing information among keypoints that are semantically related.

## 3. Method

We start with a short description of an enhanced baseline that we build on top of CapeFormer [32]. Then, we describe a graph-based approach that takes advantage of the strong graph structure available in the data. The complete architecture of our method is illustrated in Figure 2.

### 3.1. An Enhanced Baseline

We make two changes to CapeFormer architecture. First, we replace its Resnet-50 [14] backbone with a comparable-sized stronger, transformer-based, SwinV2-T [22] backbone. We also remove positional encoding because we found that it introduces an undesirable dependency on the order of the keypoints. Using these modifications, we create an **Enhanced Baseline** of the previous CapeFormer architecture. We elaborate on the impact of these changes in the experimental section.

For completeness, we give a brief description of CapeFormer, whose design is similar to the DETR architecture and consists of 4 sub-networks:

- **Shared backbone.** A pre-trained Resnet-50 is used to extract features from the input support and query images. To acquire the support keypoint features, we perform an element-wise multiplication between the support image feature map and keypoint masks. These masks are created by positioning Gaussian kernels centered at the sup-

port keypoints locations. In scenarios involving multiple support images, such as 5-shot settings, we calculate the average (in feature space) of the support keypoint features from different images. This results in both the query feature map  $\hat{F}_q \in \mathbb{R}^{hw \times C}$  and the support keypoint features  $\hat{F}_s \in \mathbb{R}^{K \times C}$ .

- **Transformer encoder.** A transformer encoder is used to fuse information between the support keypoint features and the query patch features. The encoder consists of three transformer blocks, each housing a self-attention layer. Before entering the self-attention layer, the input support keypoints and query features are concatenated and subsequently separated once more. The outputs are refined query feature map  $F_q$  and refined support keypoint features  $F_s$ .
- **Similarity-Aware Proposal Generator.** The proposal generator aligns support keypoint features with query features, resulting in similarity maps. From these maps, we select peaks to serve as the similarity-aware proposals. In pursuit of a balance between efficiency and versatility, a trainable inner-product mechanism [31] is employed to explicitly model similarity.
- **Transformer decoder.** To decode keypoint locations from the query feature map, a transformer decoder network is utilized. The Transformer decoder consists of three layers, with each layer including self-attention, cross-attention, and feed-forward blocks. An iterative refinement strategy, inspired by prior work [1, 35, 53], is applied to enable each decoder layer to predict coordinate deltas for the previous coordinate predictions. Additionally, similar to the approach in Conditional DETR [25], the decoder utilizes the predicted coordinates to provide enhanced reference points for pooling features from the image feature map.

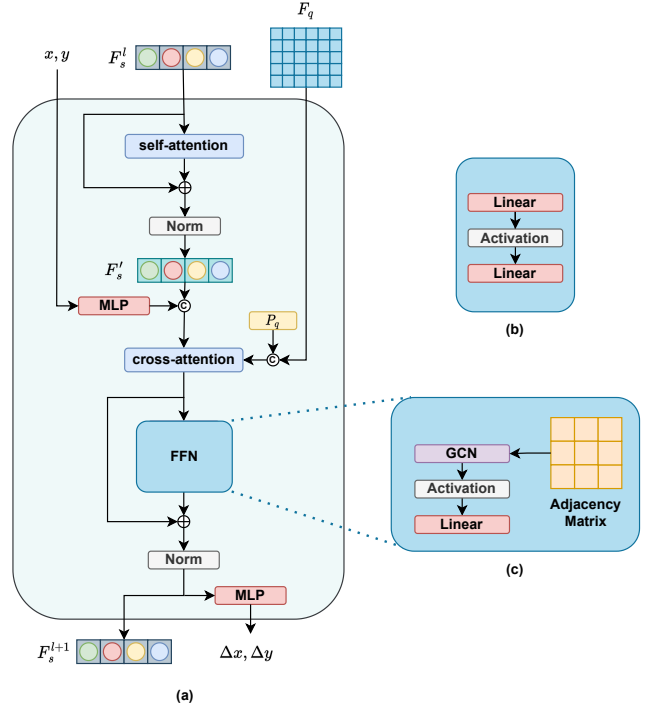


Figure 3. **Graph Transformer Decoder.** GTD is based on the original CapeFormer decoder, changing the feed-forward network from a simple MLP to a graph-based network. (a) A scheme of the transformer decoder which includes self-attention, cross-attention, and a feed-forward network. Self-attention encourages adaptive interactions among support keypoints, while cross-attention extracts localization information. (b) Previous feed-forward consisted of an MLP with 2 layers. (c) Our novel feed-forward includes a GCN layer and subsequent linear layers that enhance keypoint features and promote information exchange among known connected keypoints.

### 3.2. A Graph-Based Approach

The core idea of our work is to take advantage of the geometrical structure encoded in the pose graph. Our method is built upon the enhanced baseline, replacing the transformer decoder module with our novel Graph Transformer Decoder. We now discuss our new Graph Transformer Decoder and the associated loss function.

**Graph Transformer Decoder** We introduce a Graph Transformer Decoder (GTD) that works directly on the graph structure. As can be seen in Figure 3, GTD utilizes a novel feed-forward network in the transformer decoder layer, that includes a Graph Convolutional Network Layer (GCN).

We recognize that self-attention, a mechanism that helps our model focus on relevant information, can be thought of as a graph convolutional network (GCN) with a learnable

adjacency matrix. When we are dealing with pose estimation for a single category, this mechanism is sufficient for learning the relationships between keypoints and integrating a learned structure into the model. However, for category-agnostic pose estimation (CAPE) tasks, where the model needs to work with various object categories, it is beneficial to explicitly consider the semantic connections between keypoints. This helps the model break symmetry, maintain consistent structure, and handle noisy keypoints by sharing information among neighboring keypoints.

We implemented this prior in the transformer decoder. Specifically, GTD is based on the original CapeFormer decoder, changing the feed-forward network from a simple MLP to a GCN network. To address the potential problem of excessive smoothing often observed in deep GCNs [18, 27], which can lead to a reduction in the distinctiveness of node characteristics and consequently a decline in performance, we introduce a linear layer for each node

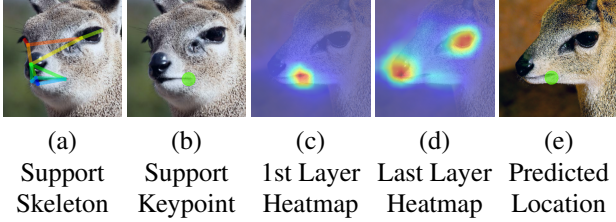


Figure 4. **Attention Map Visualization.** We illustrate the cross-attention within the decoder, specifically between  $F'_s$  and  $F_q$ . (a) illustrated the support skeleton, and (b) visualizes the searched keypoint in the support image. (c) In the initial layer, attention is centered solely on the queried keypoints. (d) In contrast, the final layer expands attention to additional keypoints based on skeletal connectivity. (e) Our decoder adeptly utilizes structural cues to accurately position keypoints within the query image.

following the GCN layer. Figure 4 illustrates the power of implementing the graph prior in the cross-attention layers. As can be seen, early layers focus on a keypoint, while later layers take into consideration also neighboring keypoints (according to the graph structure).

The original decoder has three main components: self-attention, cross-attention, and a feed-forward network. Self-attention allows for adaptive interactions among support keypoints, transforming the input feature  $F'_s$  into  $F''_s$ . Cross-attention augments support keypoints’ representation by extracting localization information from query feature patches, enhancing attention at proposed locations. This involves concatenating the keypoint localization embedding with keypoint features. Cross-attention inputs are  $F'_s$  (with the localization embedding) as queries, patch features  $F_q$  (with positional encoding) as keys, and  $F_q$  as values, resulting in transformed features  $F''_s$ . Lastly, we employ a novel feed-forward network to process the output keypoint features. To incorporate prior geometrical knowledge, we introduce a graph neural network (GCN) layer. This GCN layer further concentrates the keypoint features, facilitating the exchange of information between known keypoint connections.

The output value for an input  $F''_s \in \mathbb{R}^{C_{in} \times K}$  can be written as:

$$\widetilde{F''_s} = \sigma_{act}(W_{adj}F''_s \widetilde{A} + W_{self}F''_s) \quad (1)$$

$$F_s^{l+1} = F''_s + W_{linear}\widetilde{F''_s} \quad (2)$$

Where  $W_i \in \mathbb{R}^{C_{out} \times C_{in}}$  is a learnable parameter matrix,  $\sigma_{act}$  is an activation function (ReLU), and  $\widetilde{A} \in \mathbb{R}^{K \times K}$  is the symmetrically normalized form of the adjacency matrix  $A \in [0, 1]^{K \times K}$ , which is defined as  $a_{ij} = 1$  for node  $v_j$  that is connected to node  $v_i$  and 0 elsewhere.

The output features  $F_s^{l+1}$  are used to update the keypoints locations from  $P^l$  to  $P^{l+1}$ . We follow [32] and use

the following update function:

$$P^{l+1} = \sigma(\sigma^{-1}(P^l) + MLP(F_s^{l+1})) \quad (3)$$

where  $\sigma$  and  $\sigma^{-1}$  are the sigmoid and its inverse function. The keypoints’ positions from the last decoder layer are used as the final keypoints prediction.

**Training loss** Following CapeFormer, we use two supervision signals: a heatmap loss and an offset loss. The heatmap loss supervises the similarity metric and initial coordinates suggestion, while the offset loss supervises the localization output:

$$\mathcal{L}_{heatmap} = \frac{1}{K \cdot H \cdot W} \sum_{i=1}^K \|\sigma(M_i) - H_i\| \quad (4)$$

$$\mathcal{L}_{offset} = \frac{1}{L} \sum_{i=1}^L \sum_{i=1}^K |P_i^l - \hat{P}_i| \quad (5)$$

where  $M_i$  denotes the output similarity heatmap from the proposal generator,  $\sigma$  is the sigmoid function,  $H_i$  the ground-truth heatmap,  $P_i$  the output location from the each layer and  $\hat{P}_i$  the ground-truth location. The overall loss term is:

$$\mathcal{L} = \lambda_{heatmap} \cdot \mathcal{L}_{heatmap} + \mathcal{L}_{offset} \quad (6)$$

## 4. Experiments

We use the MP-100 dataset [42] as our training and evaluation dataset, comprising samples drawn from existing category-specific pose estimation datasets. The MP-100 dataset encompasses a collection of over 20,000 images, spanning 100 distinct categories, with varying keypoint numbers up to 68 across different categories. To facilitate model training and evaluation, the samples are divided into five distinct splits. Notably, each split ensures that training, validation, and test categories are mutually exclusive, meaning that the categories used for evaluation remain unseen during the training process.

The dataset includes partial skeleton annotations in various formats, including differences in the indexing of keypoints (some start from zero while others from one). To standardize and enhance the dataset, we adopted a unified format with comprehensive skeleton definitions for all categories. This process involved cross-referencing the original datasets and, where necessary, conducting manual annotations to ensure completeness and consistency.

To quantify our model’s performance, we employ the Probability of Correct Keypoint (PCK) metric [47], with a PCK threshold set at 0.2, following the conventions established by POMNet [42] and CapeFormer [32].

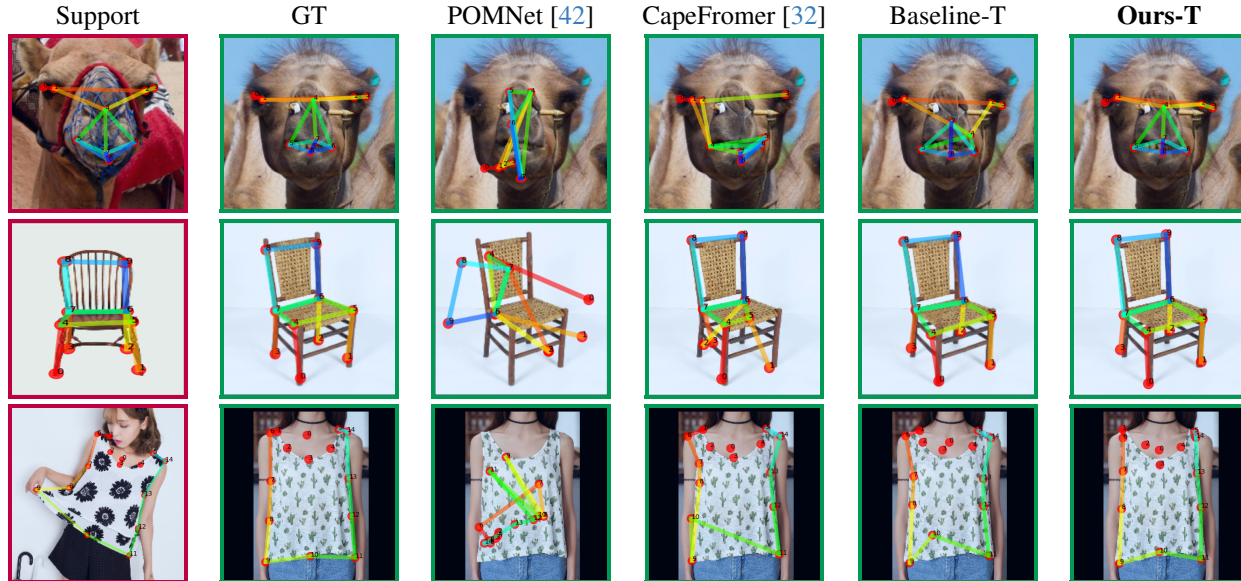


Figure 5. **Qualitative Results.** We visualize the keypoint predictions under a 1-shot setting. The left column denotes the support image with its corresponding skeleton. The second column is the ground-truth query keypoints. The following columns are results from POMNet, CapeFormer, the enhanced baseline, and our method.

We show a qualitative comparison between our method and previous CAPE methods CapeFormer [32] and POMNet<sup>1</sup> [42] in Figure 5. The last column denotes our full method, which is based on our enhanced baseline, replacing the previous decoder with our novel GTD module. As can be seen, the enhanced baseline achieves better keypoint localization than the previous state-of-the-art. Furthermore, the structure information incorporated in our method serves as a strong prior for localizing keypoints, helping in breaking symmetry and creating structure consistency between the keypoints. The first row of the figure shows an example of symmetry that confuses prior methods but not ours, while the third row shows our method’s superiority in preserving structure consistency across keypoints. More examples are in the supplementary.

#### 4.1. Implementation Details

For a fair comparison, network parameters, training parameters, and data augmentations and pre-processing are kept the same as CapeFormer [32]: Both the encoder and decoder have three layers and  $\lambda_{heatmap}$  is set to 2.0. The model is built upon MMPose framework [6], trained using Adam optimizer for 200 epochs with a batch size of 16, the learning rate is  $10^{-5}$ , and decays by 10× on the 160th and 180th epoch. More design choices and evaluations are in the supplementary.

<sup>1</sup>We used POMNet official code to train and visualize results, as they don’t provide pre-trained models. Quantitative results are taken from the published paper.

**Enhanced Backbone.** We use a stronger, transformer-based, SwinV2-T [22] backbone, instead of the original ResNet-50 [14] backbone, which can also provide a multi-scale feature map. After experimenting with various configurations, including multi-scale and single-scale feature maps, we found that applying a straightforward bilinear up-sampling on the final feature layer yielded similar results while preserving simplicity. Additionally, we optimized the extraction of support keypoint features by employing a Gaussian kernel mask with lower variance, taking advantage of the enhanced feature quality of the new backbone. These simple adjustments led to an improvement of 3.2%.

**Disable Support Keypoint Identifier.** CapeFormer introduced a keypoint positional encoding, termed the “Support Keypoint Identifier”. This encoding is generated via sinusoidal encoding of the keypoints’ order. This encoding improves performance by a significant 3% PCK, at the cost of introducing a dependency on the order of keypoints. Although the dataset contains diverse object categories, some of them share a common keypoint ordering.

This became evident when we evaluated a model trained with this positional encoding on data of keypoints in reverse order. The result was a notable decrease of approximately 30% in PCK, indicating that the model had become highly specialized for a specific keypoint format. This sharp decrease is not present when the positional encoding is not used. We believe that category-agnostic pose estimation (CAPE) should not rely on such assumptions and should ac-

commodate support keypoints without imposing a specific order. Therefore, we have chosen to remove this encoding from our baseline.

## 4.2. Benchmark Results

We compare our method with the previous CAPE methods CapeFormer [32] and POMNet [42] and three baselines: ProtoNet [33], MAML [10], and Fine-tuned [26]. Further details on these model’s evaluation can be found in [42].

We report results on the MP-100 dataset under 1-shot and 5-shot settings in Table 1. As can be seen, the enhanced baseline models, which are agnostic to the keypoints order as opposed to CapeFormer, outperform previous methods and improve the average PCK by 0.94% under the 1-shot setting and 1.60% under the 5-shot setting. Our graph-based method further improves performance, improving the enhanced baseline by 1.22% under the 1-shot setting and 0.22% under the 5-shot setting, achieving new state-of-the-art results for both settings.

We also show the scalability of our design. Similar to DETR-based models, employing a larger backbone improves performance. We show that our graph decoder design also enhances the performance of the larger enhanced baseline, improving results by 1.02% and 0.34% under 1-shot and 5-shot settings respectively.

**Out-of-Distribution Performance.** To assess the robustness of our model, we evaluate the small version of our network using images from different domains. Results are shown in Figure 6. Our model, which was trained on real images only, demonstrates its adaptability and effectiveness across varying data sources such as cartoons and imaginary animals, created using a diffusion model. Furthermore, our model demonstrates satisfactory performance even when the support and query images are from different domains.

## 4.3. Ablation Study

We conducted a number of ablation studies on the MP-100 dataset. We first evaluate our method using different backbones, showing the advantages of Swin Transformer architecture for localization tasks. We then show the contribution of the geometrical structure prior by evaluating our model using wrong skeleton relations. Lastly, we further show the power of graph structure by evaluating the performance using masked inputs. We perform all ablation experiments on the test set of MP-100 split1 under the 1-shot setting following [32, 42].

**Different Backbones.** We assess our model’s performance with various pre-trained backbones, including a CNN-based backbone (ResNet-50) and two distinct pre-trained transformer backbones, namely Dino [4, 28] and

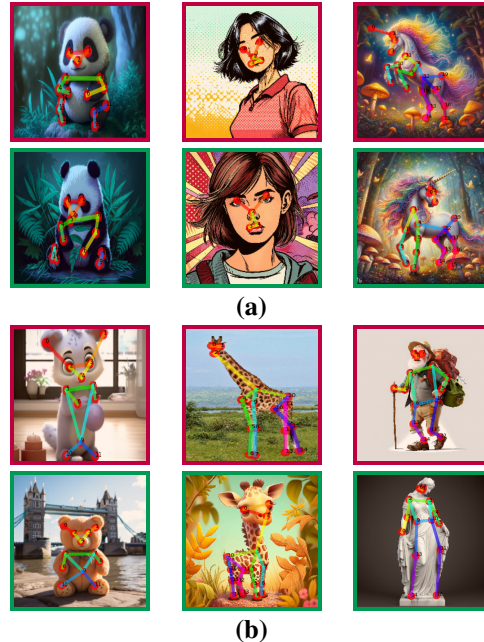


Figure 6. **Out-of-Distribution.** Qualitative results using OOD samples, **top** is the support image and **bottom** the query. **(a):** Support and query are from the same OOD domain. **(b):** Support and query images are from different domains.

Swin V2 [22]. Dino and DinoV2 are self-supervised Vision Transformers trained via self-distillation, resulting in robust, finely detailed semantic features. Moreover, these encoded semantic representations are shared among related but distinct object categories. Swin Transformer restructures self-attention with a window mechanism, balancing efficiency and performance for vision tasks. This hierarchical architecture has the flexibility to model at different scales and has linear computational complexity with respect to image size. As shown in Table 2, SwinV2 outperforms other options, delivering superior results while maintaining efficiency comparable to the CNN-based backbone. In addition, using a larger backbone boosts performance, but at the price of efficiency and size.

**The Contribution of Graph Structure.** To assess the contribution of the graph structure prior, we evaluate our method using random graph inputs by choosing edge connections randomly for each instance. This results in a performance decrease of 9.57%, validating the contribution of the graph decoder and the use of structural knowledge.

To highlight the power of graph information, we applied partial masking to the support/query image before executing our algorithm. It’s important to note that the difference between the baseline model and ours lies in the novel graph-based feed-forward network. Quantitative analysis in Figure 7a shows our method consistently outperforming the

Model	1-Shot						5-Shot					
	Split 1	Split 2	Split 3	Split 4	Split 5	Avg	Split 1	Split 2	Split 3	Split 4	Split 5	Avg
ProtoNet [33]	46.05	40.84	49.13	43.34	44.54	44.78	60.31	53.51	61.92	58.44	58.61	58.56
MAML [10]	68.14	54.72	64.19	63.24	57.20	61.50	70.03	55.98	63.21	64.79	58.47	62.50
Fine-tuned [26]	70.60	57.04	66.06	65.00	59.20	63.58	71.67	57.84	66.76	66.53	60.24	64.61
POMNet [42]	84.23	78.25	78.17	78.68	79.17	79.70	84.72	79.61	78.00	80.38	80.85	80.71
CapeFormer [32]	89.45	84.88	83.59	83.53	85.09	85.31	91.94	88.92	89.40	88.01	88.25	89.30
Baseline-T	89.48	86.69	85.31	84.79	84.97	86.25	94.04	91.20	89.19	<b>90.63</b>	89.45	90.90
<b>Ours-T</b>	<b>91.06</b>	<b>88.24</b>	<b>86.09</b>	<b>86.17</b>	<b>85.78</b>	<b>87.47</b>	<b>94.18</b>	<b>91.46</b>	<b>90.50</b>	90.18	<b>89.47</b>	<b>91.12</b>
Baseline-S	92.88	89.11	89.16	87.19	88.73	89.41	96.50	<b>92.62</b>	91.68	<b>91.23</b>	91.28	92.66
<b>Ours-S</b>	<b>93.66</b>	<b>90.42</b>	<b>89.79</b>	<b>88.68</b>	<b>89.61</b>	<b>90.43</b>	<b>96.51</b>	92.15	<b>91.99</b>	92.01	<b>92.36</b>	<b>93.00</b>

Table 1. **MP-100 Results.** PCK performance under 1-shot and 5-shot settings. In both settings, our approach consistently outperforms other methods, achieving the scores across all splits. \*-T denotes using the Tiny version of the backbone and \*-S using the Small version.

Backbone	# Params[M]	FLOPS[G]	PCK <sub>0.2</sub>
ResNet-50 [14]	25.5	4.1	87.71
DinoV1-S [4]	22.1	46.7	89.17
DinoV2-S [28]	22.1	46.7	90.34
SwinV2-T [22]	28.35	4.4	91.06
SwinV2-S [22]	49.73	8.57	93.66

Table 2. **Pre-Trained Backbone Ablation.** PCK scores using different pre-trained backbones. Swin transformer combines superior results with efficient processing.

baseline. The dashed horizontal line represents the identity operation which outputs the support keypoint’s locations, preserving structure. Notably, our model can predict keypoints even when a significant portion of the support image is masked. This suggests that the model has learned which keypoints are relevant for each category and matches them to support features based on structure. For instance, in Figure 7b (top), the model accurately predicts the sofa’s structure and most keypoints. However, when large portions of the query image are masked, the model’s performance rapidly declines, although it retains structure, as evident in Figure 7b (bottom). More examples, and additional ablation studies, can be found in the supplementary.

## 5. Conclusion

We present a novel approach for category-agnostic pose estimation (CAPE) by recognizing the importance of underlying geometrical structures within objects. We introduce a robust Graph Transformer Decoder that significantly enhances the accuracy of keypoint localization by capturing and incorporating structural information, thus exploiting the relationships and dependencies between keypoints. In addition, we provide an updated version of the MP-100 dataset, which now includes skeleton annotations for all categories, further promoting research in CAPE.

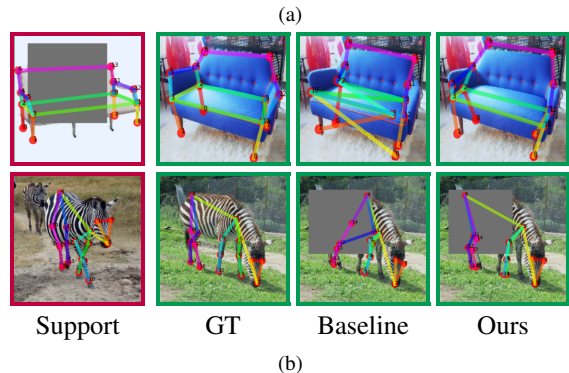
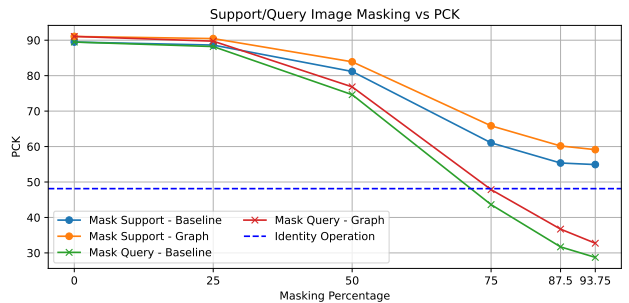


Figure 7. **Masking.** (a) Quantitative results when masking the support/query images. Our method consistently surpasses the baseline, leveraging cues provided by the graph structure to overcome information gaps in the support/query images. (b) Qualitative results when masking the support (top) and query (bottom) image using the enhanced baseline and our graph-based model.

Our experimental results demonstrate the superiority of our method over the previous state-of-the-art approach, CapeFormer, by a significant margin. With improvements under both 1-shot and 5-shot settings, our method showcases its scalability and efficiency opening the door to more versatile and adaptable applications in computer vision.

## 6. Acknowledgments

This work was partly funded by the Weinstein Institute.

## References

- [1] Zhaowei Cai and Nuno Vasconcelos. Cascade r-cnn: Delving into high quality object detection. In *Proceedings of the IEEE conference on computer vision and pattern recognition*, pages 6154–6162, 2018. 4
- [2] Z. Cao, G. Hidalgo Martinez, T. Simon, S. Wei, and Y. A. Sheikh. Openpose: Realtime multi-person 2d pose estimation using part affinity fields. *IEEE Transactions on Pattern Analysis and Machine Intelligence*, 2019. 2
- [3] Nicolas Carion, Francisco Massa, Gabriel Synnaeve, Nicolas Usunier, Alexander Kirillov, and Sergey Zagoruyko. End-to-end object detection with transformers. In *European conference on computer vision*, pages 213–229. Springer, 2020. 2
- [4] Mathilde Caron, Hugo Touvron, Ishan Misra, Hervé Jégou, Julien Mairal, Piotr Bojanowski, and Armand Joulin. Emerging properties in self-supervised vision transformers. In *Proceedings of the IEEE/CVF international conference on computer vision*, pages 9650–9660, 2021. 7, 8
- [5] Ke Cheng, Yifan Zhang, Xiangyu He, Weihang Chen, Jian Cheng, and Hanqing Lu. Skeleton-based action recognition with shift graph convolutional network. In *Proceedings of the IEEE/CVF conference on computer vision and pattern recognition*, pages 183–192, 2020. 3
- [6] MMPose Contributors. Openmmlab pose estimation toolbox and benchmark. <https://github.com/open-mmlab/mmpose>, 2020. 6
- [7] Xiyang Dai, Yinpeng Chen, Jianwei Yang, Pengchuan Zhang, Lu Yuan, and Lei Zhang. Dynamic detr: End-to-end object detection with dynamic attention. In *Proceedings of the IEEE/CVF International Conference on Computer Vision*, pages 2988–2997, 2021. 2
- [8] Hao-Shu Fang, Jiefeng Li, Hongyang Tang, Chao Xu, Haoyi Zhu, Yuliang Xiu, Yong-Lu Li, and Cewu Lu. Alpha-pose: Whole-body regional multi-person pose estimation and tracking in real-time. *IEEE Transactions on Pattern Analysis and Machine Intelligence*, 2022. 2
- [9] Yuxin Fang, Wen Wang, Binhui Xie, Quan Sun, Ledell Wu, Xinggang Wang, Tiejun Huang, Xinlong Wang, and Yue Cao. Eva: Exploring the limits of masked visual representation learning at scale. *arXiv preprint arXiv:2211.07636*, 2022. 2
- [10] Chelsea Finn, Pieter Abbeel, and Sergey Levine. Model-agnostic meta-learning for fast adaptation of deep networks. 2017. 7, 8
- [11] Peng Gao, Minghang Zheng, Xiaogang Wang, Jifeng Dai, and Hongsheng Li. Fast convergence of detr with spatially modulated co-attention. In *ICCV*, pages 3621–3630, 2021. 2
- [12] William L Hamilton, Rex Ying, and Jure Leskovec. Inductive representation learning on large graphs. In *NIPS*, pages 1025–1035, 2017. 3
- [13] Kai Han, Yunhe Wang, Jianyuan Guo, Yehui Tang, and Enhua Wu. Vision gnn: An image is worth graph of nodes. *Advances in Neural Information Processing Systems*, 35:8291–8303, 2022. 3
- [14] Kaiming He, Xiangyu Zhang, Shaoqing Ren, and Jian Sun. Deep residual learning for image recognition. In *Proceedings of the IEEE conference on computer vision and pattern recognition*, pages 770–778, 2016. 3, 6, 8
- [15] Yongcheng Jing, Yining Mao, Yiding Yang, Yibing Zhan, Mingli Song, Xinchao Wang, and Dacheng Tao. Learning graph neural networks for image style transfer. In *ECCV*, 2022. 3
- [16] Sven Kreiss, Lorenzo Bertoni, and Alexandre Alahi. Openpipaf: Composite fields for semantic keypoint detection and spatio-temporal association. *IEEE Transactions on Intelligent Transportation Systems*, 23(8):13498–13511, 2021. 2
- [17] Loic Landrieu and Martin Simonovsky. Large-scale point cloud semantic segmentation with superpoint graphs. In *CVPR*, pages 4558–4567, 2018. 3
- [18] Qimai Li, Zhichao Han, and Xiao-Ming Wu. Deeper insights into graph convolutional networks for semi-supervised learning. In *Proceedings of the AAAI conference on artificial intelligence*, 2018. 4
- [19] Kevin Lin, Lijuan Wang, and Zicheng Liu. End-to-end human pose and mesh reconstruction with transformers. In *IEEE CVPR*, pages 1954–1963, 2021. 3
- [20] Shilong Liu, Feng Li, Hao Zhang, Xiao Yang, Xianbiao Qi, Hang Su, Jun Zhu, and Lei Zhang. Dab-detr: Dynamic anchor boxes are better queries for detr. *arXiv preprint arXiv:2201.12329*, 2022. 2
- [21] Ziyu Liu, Hongwen Zhang, Zhenghao Chen, Zhiyong Wang, and Wanli Ouyang. Disentangling and unifying graph convolutions for skeleton-based action recognition. In *Proceedings of the IEEE/CVF conference on computer vision and pattern recognition*, pages 143–152, 2020. 3
- [22] Ze Liu, Han Hu, Yutong Lin, Zhuliang Yao, Zhenda Xie, Yixuan Wei, Jia Ning, Yue Cao, Zheng Zhang, Li Dong, et al. Swin transformer v2: Scaling up capacity and resolution. In *Proceedings of the IEEE/CVF conference on computer vision and pattern recognition*, pages 12009–12019, 2022. 3, 6, 7, 8
- [23] Weian Mao, Yongtao Ge, Chunhua Shen, Zhi Tian, Xinlong Wang, and Zhibin Wang. Tfpose: Direct human pose estimation with transformers. *arXiv preprint arXiv:2103.15320*, 2021. 2
- [24] Depu Meng, Xiaokang Chen, Zejia Fan, Gang Zeng, Houqiang Li, Yuhui Yuan, Lei Sun, and Jingdong Wang. Conditional detr for fast training convergence. In *Proceedings of the IEEE International Conference on Computer Vision (ICCV)*, 2021. 2
- [25] Depu Meng, Xiaokang Chen, Zejia Fan, Gang Zeng, Houqiang Li, Yuhui Yuan, Lei Sun, and Jingdong Wang. Conditional detr for fast training convergence. In *Proceedings of the IEEE/CVF International Conference on Computer Vision*, pages 3651–3660, 2021. 4
- [26] Akihiro Nakamura and Tatsuya Harada. Revisiting fine-tuning for few-shot learning. *arXiv preprint arXiv:1910.00216*, 2019. 7, 8
- [27] Kenta Oono and Taiji Suzuki. Graph neural networks exponentially lose expressive power for node classification. *arXiv preprint arXiv:1905.10947*, 2019. 4

- [28] Maxime Oquab, Timothée Darcet, Théo Moutakanni, Huy Vo, Marc Szafraniec, Vasil Khalidov, Pierre Fernandez, Daniel Haziza, Francisco Massa, Alaaeldin El-Nouby, et al. Dinov2: Learning robust visual features without supervision. *arXiv preprint arXiv:2304.07193*, 2023. 7, 8
- [29] N Dinesh Reddy, Minh Vo, and Srinivasa G Narasimhan. Carfusion: Combining point tracking and part detection for dynamic 3d reconstruction of vehicles. In *Proceedings of the IEEE conference on computer vision and pattern recognition*, pages 1906–1915, 2018. 2
- [30] Prithviraj Sen, Galileo Namata, Mustafa Bilgic, Lise Getoor, Brian Gallagher, and Tina Eliassi-Rad. Collective classification in network data. *AI magazine*, 29(3):93–93, 2008. 3
- [31] Min Shi, Hao Lu, Chen Feng, Chengxin Liu, and Zhiguo Cao. Represent, compare, and learn: A similarity-aware framework for class-agnostic counting. In *Proceedings of the IEEE/CVF Conference on Computer Vision and Pattern Recognition*, pages 9529–9538, 2022. 4
- [32] Min Shi, Zihao Huang, Xianzheng Ma, Xiaowei Hu, and Zhiguo Cao. Matching is not enough: A two-stage framework for category-agnostic pose estimation. In *Proceedings of the IEEE/CVF Conference on Computer Vision and Pattern Recognition (CVPR)*, pages 7308–7317, 2023. 2, 3, 5, 6, 7, 8
- [33] Jake Snell, Kevin Swersky, and Richard Zemel. Prototypical networks for few-shot learning. *NeurIPS*, 2017. 2, 7, 8
- [34] Xibin Song, Peng Wang, Dingfu Zhou, Rui Zhu, Chenye Guan, Yuchao Dai, Hao Su, Hongdong Li, and Ruigang Yang. Apollocar3d: A large 3d car instance understanding benchmark for autonomous driving. In *Proceedings of the IEEE/CVF Conference on Computer Vision and Pattern Recognition*, pages 5452–5462, 2019. 2
- [35] Zachary Teed and Jia Deng. Raft: Recurrent all-pairs field transforms for optical flow. In *Computer Vision–ECCV 2020: 16th European Conference, Glasgow, UK, August 23–28, 2020, Proceedings, Part II 16*, pages 402–419. Springer, 2020. 4
- [36] Petar Veličković, Guillem Cucurull, Arantxa Casanova, Adriana Romero, Pietro Lio, and Yoshua Bengio. Graph attention networks. *arXiv preprint arXiv:1710.10903*, 2017. 3
- [37] Nikil Wale, Ian A Watson, and George Karypis. Comparison of descriptor spaces for chemical compound retrieval and classification. *Knowledge and Information Systems*, 14(3):347–375, 2008. 3
- [38] Runzhong Wang, Junchi Yan, and Xiaokang Yang. Learning combinatorial embedding networks for deep graph matching. In *ICCV*, pages 3056–3065, 2019. 3
- [39] Wenhai Wang, Jifeng Dai, Zhe Chen, Zhenhang Huang, Zhiqi Li, Xizhou Zhu, Xiaowei Hu, Tong Lu, Lewei Lu, Hongsheng Li, et al. Internimage: Exploring large-scale vision foundation models with deformable convolutions. *arXiv preprint arXiv:2211.05778*, 2022. 2
- [40] Yue Wang, Yongbin Sun, Ziwei Liu, Sanjay E Sarma, Michael M Bronstein, and Justin M Solomon. Dynamic graph cnn for learning on point clouds. *Acm Transactions On Graphics (tog)*, 38(5):1–12, 2019. 3
- [41] Danfei Xu, Yuke Zhu, Christopher B Choy, and Li Fei-Fei. Scene graph generation by iterative message passing. In *CVPR*, pages 5410–5419, 2017. 3
- [42] Lumin Xu, Sheng Jin, Wang Zeng, Wentao Liu, Chen Qian, Wanli Ouyang, Ping Luo, and Xiaogang Wang. Pose for everything: Towards category-agnostic pose estimation. In *European Conference on Computer Vision*, pages 398–416. Springer, 2022. 2, 5, 6, 7, 8
- [43] Yufei Xu, Jing Zhang, Qiming Zhang, and Dacheng Tao. Vit-pose: Simple vision transformer baselines for human pose estimation. *Advances in Neural Information Processing Systems*, 35:38571–38584, 2022. 2
- [44] Sijie Yan, Yuanjun Xiong, and Dahua Lin. Spatial temporal graph convolutional networks for skeleton-based action recognition. In *AAAI*, 2018. 3
- [45] Jianwei Yang, Jiasen Lu, Stefan Lee, Dhruv Batra, and Devi Parikh. Graph r-cnn for scene graph generation. In *ECCV*, pages 670–685, 2018. 3
- [46] Sen Yang, Zhibin Quan, Mu Nie, and Wankou Yang. Transpose: Keypoint localization via transformer. In *Proceedings of the IEEE/CVF International Conference on Computer Vision*, pages 11802–11812, 2021. 2
- [47] Yi Yang and Deva Ramanan. Articulated human detection with flexible mixtures of parts. *IEEE transactions on pattern analysis and machine intelligence*, 35(12):2878–2890, 2012. 5
- [48] Yuxiang Yang, Junjie Yang, Yufei Xu, Jing Zhang, Long Lan, and Dacheng Tao. Apt-36k: A large-scale benchmark for animal pose estimation and tracking. *Advances in Neural Information Processing Systems*, 35:17301–17313, 2022. 2
- [49] Hang Yu, Yufei Xu, Jing Zhang, Wei Zhao, Ziyu Guan, and Dacheng Tao. Ap-10k: A benchmark for animal pose estimation in the wild. In *Thirty-fifth Conference on Neural Information Processing Systems Datasets and Benchmarks Track (Round 2)*, 2021. 2
- [50] Hao Zhang, Feng Li, Shilong Liu, Lei Zhang, Hang Su, Jun Zhu, Lionel M Ni, and Heung-Yeung Shum. Dino: Detr with improved denoising anchor boxes for end-to-end object detection. *arXiv preprint arXiv:2203.03605*, 2022. 2
- [51] Long Zhao, Xi Peng, Yu Tian, Mubbasir Kapadia, and Dimitris N Metaxas. Semantic graph convolutional networks for 3d human pose regression. In *IEEE CVPR*, pages 3425–3435, 2019. 3
- [52] Weixi Zhao, Weiqiang Wang, and Yunjie Tian. Graformer: Graph-oriented transformer for 3d pose estimation. In *Proceedings of the IEEE/CVF Conference on Computer Vision and Pattern Recognition*, pages 20438–20447, 2022. 3
- [53] Xizhou Zhu, Weijie Su, Lewei Lu, Bin Li, Xiaogang Wang, and Jifeng Dai. Deformable detr: Deformable transformers for end-to-end object detection. *arXiv preprint arXiv:2010.04159*, 2020. 2, 4